SPANDIDOS PUBLICATIONS

INTERNATIONAL JOURNAL OF ONCOLOGY 54: 177-187, 2019

miR-34a regulates the chemosensitivity of retinoblastoma cells via modulation of MAGE-A/p53 signaling

GE YANG[1*], YANG FU[2*], XIAOYAN LU[1], MENGHUA WANG[1], HONGTAO DONG[1] and QIUMING LI[1]

Departments of [1]Ophthalmology and [2]General Surgery, The First Affiliated Hospital of Zhengzhou University, Zhengzhou, Henan 450052, P.R. China

Received March 9, 2018; Accepted June 22, 2018

DOI: 10.3892/ijo.2018.4613

Abstract. The present study aimed to explore the combined role of microRNA (miR)-34a, melanoma antigen-A (MAGE-A) and p53 in altering the chemosensitivity of retinoblastoma (RB) cells. Human RB and adjacent tumor tissues, as well as human RB cell lines (HXO-Rb44, SO-Rb50, Y79 and WERI-Rb-1) were used. In addition, four chemotherapeutic drugs, including carboplatin, etoposide, Adriamycin and vincristine, were used to treat the cell lines, in order to evaluate the sensitivity of RB cells. Furthermore, miR-34a expression was detected by reverse transcription-quantitative polymerase chain reaction, and western blotting was implemented to quantify expression levels of MAGE-A and p53. A luciferase reporter gene assay was used to validate the targeted association between miR-34a and MAGE-A. The results indicated that SO-Rb50 cells exhibited the highest resistance to carboplatin, Adriamycin and vincristine ($P<0.05$), whereas HXO-Rb44 cells revealed the highest inhibition rate in response to etoposide ($P<0.05$) out of the four cell lines. Furthermore, reduced miR-34a expression and increased MAGE-A expression significantly elevated the survival rate and viability of SO-Rb50 cells following drug treatment (all $P<0.05$). miR-34a was also demonstrated to directly target MAGE-A, thereby significantly promoting the viability of RB cells and depressing apoptosis ($P<0.05$). p53, which was subjected to modulation by miR-34a and MAGE-A, also significantly reduced the proliferation rate of RB cells ($P<0.05$). In conclusion, the miR-34a/MAGE-A/p53 axis may be conducive to enhancing the efficacies of chemotherapeutic treatments for RB.

Correspondence to: Dr Ge Yang or Dr Qiuming Li, Department of Ophthalmology, The First Affiliated Hospital of Zhengzhou University, 1 Jianshe East Road, Zhengzhou, Henan 450052, P.R. China
E-mail: dd_yangge056@126.com
E-mail: liqiuminghn@163.com

*Contributed equally

Key words: retinoblastoma, microRNA-34a, melanoma antigen-A, p53, chemosensitivity, cell viability, cell apoptosis

Introduction

Retinoblastoma (RB), is the most common type of primary ocular malignant tumor in infants, with a worldwide incidence of ~1/20,000 cases (1). Up to 1,000 new RB cases are diagnosed each year in China, which accounts for ~20% of cases worldwide (2). Notably, pediatric patients are likely to succumb within the 1-2 years following RB onset if no treatments are received (3). To relieve the symptoms of RB, various therapies have been developed, in particular, chemotherapy followed by adjuvant therapy has been gradually prioritized considering the severe complications caused by other treatment strategies (4,5). However, as drug resistance is a major reason for treatment failure or RB recurrence, numerous studies have attempted to identify novel biomarkers for RB (6-8).

It has been documented that the expression of various microRNAs (miRNAs/miRs) are abnormally expressed within neoplastic tissues and cells (9). Among them, miR-34a was demonstrated to induce cell apoptosis, delay cell cycle progression and encourage cell senescence, which are considered important characteristics of tumor onset and aggravation (10-13). Furthermore, miR-34 was demonstrated to facilitate the onset and development of colorectal cancer through regulating DNA methylation (14). This miRNA also blocks epidermal growth factor receptor (EGFR) signaling by modifying phosphoinositide 3-kinase, ultimately contributing to the inhibition of gastric cancer progression (15). Notably, downregulated miR-34a expression induces the multiplication of RB cells (16), though the underlying mechanisms remain unclear.

Numerous studies have confirmed that miR-34a serves an important role in regulating tumor cell sensitivity to chemotherapeutic drugs, and this effect may be primarily associated with the post-transcriptional regulation of oncogenes by miR-34a (17-19). For instance, Vinall *et al* (20) reported that miR-34a increases the sensitivity of bladder cancer cells to cisplatin by inhibiting the expression levels of cyclin dependent kinase 6 and sirtuin 1. It has also suggested that miR-34a may affect the expression of various drug-resistant proteins within tumor cells by altering the Notch1 signaling pathway (21) Notably, the combined effect of miR-34a and melanoma antigen-A (MAGE-A) on the chemosensitivity of tumor cells has been confirmed (22). Furthermore, the

MAGE-A family proteins have been demonstrated to be involved in guide cell carcinogenesis by interfering with the p53 signaling pathway and thereby reduce the sensitivity of tumor cells to chemotherapeutic drugs (23,24). Nevertheless, few studies have focused on the associations among miR-34a, MAGE-A and p53 underlying the chemosensitivity of RB (1).

The present study aimed to investigate the involvement of the miR-34a/MAGE-A/p53 signaling pathway on the sensitivity of RB to chemotherapeutic drugs using tissue samples and *in vitro* experiments, which may provide a basis for clinically diagnosing and treating RB in the future.

Materials and methods

Collection of tissues. A total of 293 RB and adjacent tumor tissue samples were collected from the Department of Ophthalmology, The First Affiliated Hospital of Zhengzhou University between April 2015 and January 2017. The mean age of patients was 23.64±17.04 months (11-61 months), with 155 females and 138 males. Notably, only infants <6 years old were included, and patients with family heredity were excluded. All the tissues were fixed with 4% paraformaldehyde at room temperature for 30 min, and were surgically diagnosed as RB by ≥2 senior pathologists who were blinded to the clinicopathological features of patients. The immediate relatives of all patients with RB provided written informed consent, and the present study was approved by the Ethics Committee of The First Affiliated Hospital of Zhengzhou University.

Cultivation of RB cells and cell transfection. Human RB cell lines, HXO-Rb44, SO-Rb50, Y79 and WERI-Rb-1, were purchased from the American Type Culture Collection (Manassas, VA, USA). The cells were cultured with RMPI-1640 supplemented with 10% fetal calf serum (both from Invitrogen; Thermo Fisher Scientific, Inc., Waltham, MA, USA) in a humidified atmosphere with 5% CO_2. The culture medium was replaced every 3-4 days, and all cell lines were maintained within 20 generations. When the confluence of RB cells reached ~50%, the Lipofectamine™ 2000 Liposome Transfection kit (Invitrogen; Thermo Fisher Scientific, Inc.) was used to transfect cells. The following oligonucleotides were used: miR-34a mimics (40 nM) forward, 5'-UGGCAGUGUCUUAGCUGGUUGU-3' and reverse, 5'-AACCAGCUAAGACACUGCCAUU-3'; miR-34a inhibitor (40 nM) forward, 5'-ACAACCAGCUAAGACACUGCCA-3' and reverse, 5'-UGGCAGUGUCUUAGCUGGUUGU-3'; miR-negative control (NC) (40 nM) forward, 5'-CAGUACUUUUGUGUAGUACAA-3' and reverse, 5'-UUGUACUACACAAAAGUACUG-3'; pcDNA3.1-MAGE-A (30 nM); small interfering RNA (si)-MAGE-A 3/6/12 (30 nM) forward, 5'-CUACCUGGAGUACCGGCAG-3' and reverse, 5'-UGGCAGUGUCUUAGCUGGUUGU-3'; pcDNA3.1-p53 (30 nM) or si-p53 (30 nM) forward, 5'-GAAGAAAAUUUCCGCAAAA-3' and reverse, 5'-CUU UUGCGGAAAUUUUCUUC-3' (all from Guangzhou RiboBio Co., Ltd., Guangzhou, China).

Reverse transcription-quantitative polymerase chain reaction (RT-qPCR). Tissues and cells were lysed with addition of 1 ml TRIzol solution (Invitrogen; Thermo Fisher Scientific, Inc.), and total RNA was extracted according to the manufacturer's protocol. The purity and concentration of RNA were determined using spectrophotometry. Subsequently, the extracted RNA was reverse transcribed into cDNA, and amplified using PCR according to the PrimeScript one-step RT-qPCR kit (Takara Bio, Inc., Otsu, Japan) protocol. The temperature protocol for RT was as follows: 16˚C for 30 min; 42˚C for 30 min; and 85˚C for 5 min. ABI Primer Express software (version 2.0; Guangzhou RiboBio Co., Ltd.) was used to design the primers (Table I). The primers were added to the 25 μl PCR reaction system, and the reaction conditions were as follows: Pre-denaturation at 95˚C for 2 min; and 30 cycles of denaturation at 94˚C for 45 sec, renaturation at 59˚C for 45 sec and extension at 72˚C for 30 sec. The expression levels of miR-34a, MAGE-A and p53 were determined using a CFX96™ thermocycler (Bio-Rad Laboratories, Inc., Hercules, CA, USA), and quantified according to the comparative Cq method ($2^{-\Delta\Delta Cq}$) (4). U6 was designated as the internal reference for miR-34a, and β-actin was adopted as the internal reference for MAGE-A and p53.

Table I. Primers for miR-34a, MAGE-A, p53, U6 and β-actin used in RT-qPCR.

Genes	Primer sequence
miR-34a	
Forward	5'-CGGTATCATTTGGCAGTGTCT-3'
Reverse	5'-GTGCAGGGTCCGAGGT-3'
U6	
Forward	5'-CTCGCTTCGGCAGCACA-3'
Reverse	5'-AACGCTTCACGAATTTGCGT-3'
MAGE-A	
Forward	5'-ATGGAGACTCAGTTCCGAGA-3'
Reverse	5'-AAGAACTTTCATCTTGCTGG-3'
p53	
Forward	5'-CTGCCCTCAACAAGATGTTTTG-3'
Reverse	5'-CTATCTGAGCAGCGCTCATGG-3'
β-actin	
Forward	5'-CTTAGTTGCGTTACACCCTTTCTTG-3'
Reverse	5'-CTGTCACCTTCACCGTTCCAGTTT-3'

MAGE-A, melanoma antigen-A; miR-34a, microRNA-34a; RT-qPCR, reverse transcription-quantitative polymerase chain reaction.

Luciferase reporter gene assay. The MAGE-A fragments that contained binding sites of miR-34a were amplified by PCR, and were then cloned into pmirGLO double luciferase expression vector (Promega Corporation, Madison, WI, USA) to form MAGE-A-wt. Through a similar approach, MAGE-A-mut was constructed, except that the binding sites of miR-34a within MAGE-A were mutated. Subsequently, RB cells that were transfected with MAGE-A-wt, MAGE-A-mut or pRL-TK reporter gene vector were transfected with miR-34a mimic, miR-34a inhibitor or miR-NC using Lipofectamine 2000. The resultant firefly luciferase and Renilla luciferase activity were measured using a Double Luciferase Reporter assay system (Promega Corporation) following 24 h of transfection.

Western blotting. Total protein was extracted using immunoprecipitation assay lysis buffer (Beyotime Institute of Biotechnology, Haimen, China) and quantified using the Bradford method. Each sample (40 μg) was separated using 8% SDS-PAGE and then transferred onto polyvinylidene fluoride membranes. Following blocking with 50 g/l skim milk powder for 1.5 h at room temperature, bovine serum albumin was added to diluted primary antibodies against MAGE-A (mouse anti-human; 1:500; Santa Cruz Biotechnology, Inc., Dallas, TX, USA; cat. no. sc-20034) and p53 (mouse anti-human; 1:500; Sigma-Aldrich; Merck KGaA, Darmstadt, Germany; cat. no. P5813), E-cadherin, N-cadherin, vimentin, snail (mouse anti-human; 1:1,000; Abcam, Cambridge, UK; cat. nos. ab76055, ab98952, ab8978 and ab82846, respectively) and GAPDH (rabbit anti-human; 1:1,000; Santa Cruz Biotechnology, Inc.; cat. no. sc-47724). After the samples were incubated at 4˚C overnight, the membranes were washed with 1 ml/l TBS-Tween-20 three times. Then, the rabbit anti-mouse IgG H&L (DyLight® 550) preadsorbed secondary antibody (1:5,000; Abcam; cat. no. ab98786) was added, and the membranes were incubated at room temperature for 2 h. Finally, GelDoc2000 Enhanced Chemiluminescence reagent (Bio-Rad Laboratories, Inc.) was used for development in the darkroom, and the expression levels of the aforementioned proteins were assessed using ImageJ software (version 1.46; National Institutes of Health, Bethesda, MD, USA) was employed to analyze the protein bands.

Evaluation of drug susceptibility. A 100 μl cell suspension at the density of $4x10^3$/ml was added into each well of the 96-well plates. When cells adhered to the wall, the following drug treatments were performed: Vincristine (0.05, 0.10, 0.50, 1.00 and 5.00 μg/ml), etoposide (0.5, 1.0, 5.0, 10.0 and 50.0 μg/ml), carboplatin (1.5, 7.5, 15.0, 75.0 and 150.0 μg/ml), and Adriamycin (1.0, 5.0, 10.0, 50.0 and 100.0 μg/ml) (all from Sigma-Aldrich; Merck KGaA). Subsequently, the samples were agitated and cultured at 37˚C for 48 h in 5% CO_2. Then, 0.5% MTT (10 μl) was added to each well and incubated at 37˚C for 4-6 h in 5% CO_2. Following the removal of the supernatant from the wells, each well was supplemented with 100 μl acidulated isopropanol. Following culturing at room temperature for 15-30 min, the samples were detected based on the optical density (OD) values at 570 nm using a Freedom Evolyzer-2200 Enzyme-Linked Immunometric meter (Tecan Group Ltd., Männedorf, Switzerland). Finally, the inhibition rate (IR, %) was calculated according to the formula as follows: [1- ($OD_{medicine}$ / $OD_{control}$)] x 100. The drug concentration that caused death of half of the cells also known as the half maximal inhibitory concentration (IC_{50}), was also calculated.

Cell apoptosis analysis. The cells were washed with 0.01 mol/l PBS, and were centrifuged at 1,500 x g for 5 min at 4˚C. The supernatant was discarded, and 500 μl 1X binding buffer (Thermo Fisher Scientific, Inc.) was added to adjust the concentration of cells to $1x10^6$/ml. Subsequently, the cells in each tube were mixed with 500 μl cell suspension, 5 μl Annexin V-fluorescein isothiocyanate and 10 μl propidium iodide (Invitrogen; Thermo Fisher Scientific, Inc.). Following the incubation of the cells at room temperature for 10 min, the samples were analyzed using a FACSCalibur flow cytometer with CellQuest software (version 3.3; both from BD Biosciences, Franklin Lakes, NJ, USA).

Statistical analysis. All data were analyzed using SPSS 13.0 statistical software (SPSS, Inc., Chicago, IL, USA). The results are expressed as the mean ± standard deviation. All the experiments were repeated for at least three times. Differences between two groups were analyzed using the Student's t-test, and those of ≥3 groups were compared using one-way analysis of variance with the Student-Newman-Keuls post hoc test. As for the categorical data (n, %), the χ^2 test was used for analysis. Spearman's correlation analysis was also performed to assess the associations among miR-34a, MAGE-A and p53 expression. The Kaplan-Meier estimator method was applied to calculate overall survival of the studied population, and the log-rank test was used to evaluate the significance of differences. Cox regression model was used to perform univariate and multivariate analyses. Furthermore, in order to investigate the role of miR-34a and MAGE-A underlying RB etiology, their binding sites were predicted using the Targetscan database (http://www. targetscan.org/). P<0.05 was considered to indicate a statistically significant difference.

Results

miR-34a, MAGE-A and p53 expression levels in human RB tissues and cell lines. RT-qPCR was used to detect the expression levels of MAGE-A, p53 and miR-34a within human RB tissues and paracarcinoma tissues. MAGE-A and p53 expression levels within RB tissues were significantly upregulated compared with paracarcinoma tissues (P<0.01); however, the expression of miR-34a was significantly downregulated in RB tissues (P<0.01) (Fig. 1A). Further analyses demonstrated that miR-34a expression was negatively correlated with MAGE-A expression in the investigated RB tissues (r_s -0.51; P<0.001), and positively correlated with p53 expression (r_s, 0.61; P<0.001) (Fig. 1B). In addition, a negative correlation was identified between MAGE-A and p53 expression levels among the collected RB samples (r_s, -0.33; P<0.001).

The patients with RB were divided into the high miR-34a expression (≥0.48) and low miR-34a expression groups (<0.48) (Table II). Patients were also divided into high and low MAGE-A expression groups using the mean overall expression (1.97) as a threshold. It was indicated that low miR-34a and high MAGE-A expression were significantly associated with higher stages (D-E) of the International Classification of Retinoblastoma (ICRB) system (5) (χ^2, 4.67; P=0.031; χ^2, 58.92; P<0.001), poor differentiation (χ^2, 7.76; P=0.005; χ^2, 8.87; P=0.003), positive choroidal invasion (χ^2, 6.21; P=0.013; χ^2, 4.53; P=0.033) and positive optic nerve involvement (χ^2, 7.92; P=0.005; χ^2, 9.52; P=0.002), when compared with the high miR-34a and low MAGE-A expression groups (Table II). However, no significant associations were identified between the two genes, and age, sex, family history or eye effected. In addition, Kaplan-Meier estimator analyses demonstrated that patients with RB with low miR-or high MAGE-A expression were associated with significantly lower overall survival rates compared with the high miR-34a or low

Table II. Association between microRNA-34a and MAGE-A expression levels, and the clinical characteristics of patients with RB.

	microRNA-34a expression				MAGE-A expression			
Characteristics	Low	High	χ^2	P-value	Low	High	χ^2	P-value
Total (n=293)	213	80			88	205		
Age, months								
<30	137	57	1.25	0.264	60	134	0.22	0.640
≥30	76	23			28	71		
Sex								
Female	112	43	0.03	0.858	45	110	0.16	0.692
Male	101	37			43	95		
Family history								
Negative	175	71	1.88	0.171	77	169	1.17	0.279
Positive	38	9			11	36		
Eye affected								
Right	105	45	1.13	0.289	46	104	0.06	0.809
Left	108	35			42	101		
ICRB staging system								
Group A-C	82	42	4.67	0.031	67	57	58.92	<0.001
Group D-E	131	38			21	148		
Degree of differentiation								
Well and moderately	122	60	7.76	0.005	66	116	8.87	0.003
Poorly	91	20			22	89		
Choroidal invasion								
Negative	101	51	6.21	0.013	54	98	4.53	0.033
Positive	112	29			34	107		
Scleral invasion								
Negative	193	78	3.98	0.046	84	187	1.59	0.207
Positive	20	2			4	18		
Optic nerve involvement								
Negative	86	47	7.92	0.005	52	81	9.52	0.002
Positive	127	33			36	124		

MAGE-A, melanoma antigen-A; RB, retinoblastoma; miR-34a, microRNA-34a; ICRB, International Classification of Retinoblastoma.

MAGE-A expression groups (P<0.05; Fig. 1C). Multivariate Cox regression analysis demonstrated that low miR-34a expression [hazard ratio (HR), 2.10; 95% confidence interval (CI), 1.10-4.02; P=0.025], high MAGE-A expression (HR, 2.13; 95% CI, 1.04-4.17; P=0.037), stage D-E of the ICRB system (HR, 1.89; 95% CI, 1.04-3.45; P=0.037), poor differentiation (HR, 1.75; 95% CI, 1.02-2.94; P=0.040) and optic nerve involvement (HR, 1.92; 95% CI, 1.11-3.23; P=0.019) were independent prognostic factors for RB (Table III).

Sensitivities to carboplatin, etoposide, Adriamycin and vincristine in HXO-Rb44, SO-Rb50, Y79 and WERI-RB1 cell lines. The results of the MTT assay revealed that SO-Rb50 cells exhibited a maximal sensitivity to carboplatin (IC_{50}, 17.43 μg/ml) and Adriamycin (IC_{50}, 5.49 μg/ml) (Fig. 2A-C). Furthermore, the inhibitory response to etoposide were ranked as follows: Y79 (IC_{50}, 20.96 μg/ml) > SO-Rb50 (IC_{50}, 20.84 μg/ml) > WERI-RB1 (IC_{50}, 9.73 μg/ml) > HXO-Rb44 (IC_{50}, 4.92 μg/ml) (Fig. 2B). Y79 (IC_{50}, 0.07 μg/ml) and SO-Rb50 (IC_{50}, 0.0.11 μg/ml) exhibited higher sensitivity to vincristine compared with WERI-RBI (IC_{50}, 0.46 μg/ml) and HXO-Rb44 (IC_{50}, 0.51 μg/ml) (Fig. 2D). Furthermore, miR-34a and p53 expression levels were highest in SO-Rb50 cells out of all four cell lines (P<0.05; Fig. 2E). MAGE-A expression in HXO-Rb50 and SO-Rb50 were the lowest among all the cell lines (P<0.05). Thus, SO-Rb50 was selected for the following experiments.

miR-34a and MAGE-A regulate the viability and apoptosis of RB cells. The SO-Rb50 cells were treated with 17.43 μg/ml carboplatin, 20.84 μg/ml etoposide, 5.49 μg/ml Adriamycin or 0.11 μg/ml vincristine. It was demonstrated that the survival rates of SO-Rb50 were significantly inhibited following miR-34a mimics transfection (P<0.05), while silencing of miR-34a appeared to significantly increase the survival rate of SO-Rb50 cells compared with the NC group (P<0.05) (Fig. 3A).

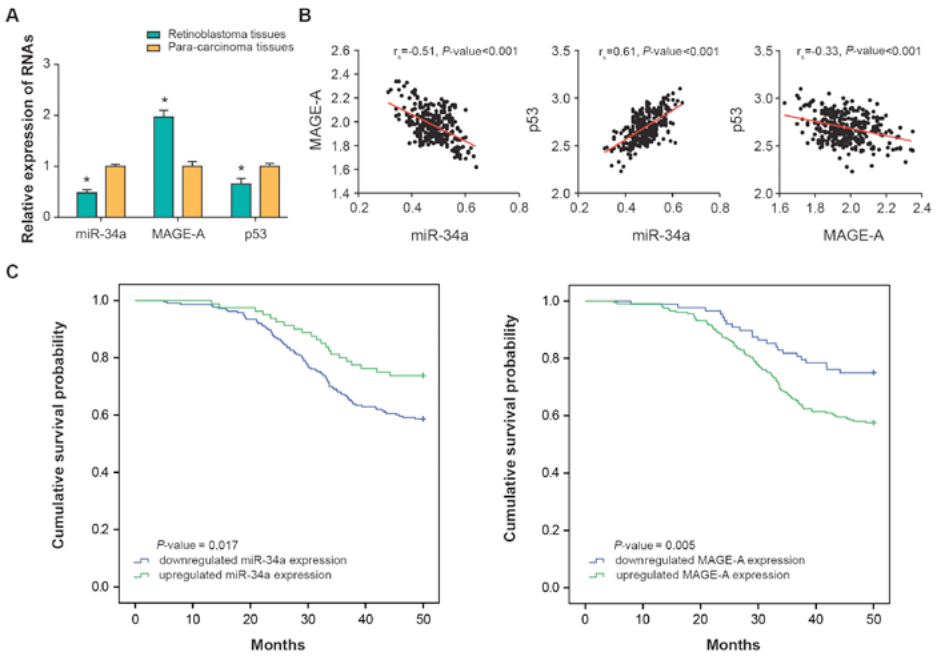

Figure 1. Expression levels of miR-34a, MAGE-A and p53 in retinoblastoma tissues and cells. (A) miR-34a, MAGE-A and p53 expression levels were compared between retinoblastoma tissues and adjacent non-tumor tissues. *P<0.05 compared with adjacent non-tumor tissues. (B) Correlation analyses were performed among miR-34a, MAGE-A and p53. (C) The survival rates of patients with retinoblastoma with differentially expressed miR-34a and MAGE-A were compared. MAGE-A, melanoma antigen-A; miR-34a, microRNA-34a.

Table III. Association between clinical characteristics and the overall survival of patients with RB.

	Univariate analysis			Multivariate analysis		
Characteristics	HR	95% CI	P-value	HR	95% CI	P-value
miRNA-34a expression						
Low vs. high	2.57	1.42-4.64	0.002	2.1	1.10-4.02	0.025
MAGE-A expression						
Low vs. high	3.45	1.89-6.25	<0.001	2.13	1.04-4.17	0.037
Age, months						
<30 vs. ≥30	1.13	0.68-1.87	0.64	1.33	0.76-2.33	0.320
Sex						
Female vs. male	0.96	0.60-1.55	0.873	1.03	0.61-1.75	0.905
Family history						
Positive vs. negative	0.76	0.39-1.47	0.414	0.56	0.27-1.19	0.131
Eye affected						
Right vs. left	0.85	0.53-1.36	0.498	0.93	0.55-1.58	0.794
ICRB staging system						
Group D-E vs. group A-C	2.78	1.64-4.55	<0.001	1.89	1.04-3.45	0.037
Degree of differentiation						
Poorly vs. well/moderately	2.33	1.43-3.85	0.001	1.75	1.02-2.94	0.040
Choroidal invasion						
Positive vs. negative	1.96	1.22-3.23	0.005	1.64	0.97-2.78	0.065
Scleral invasion						
Positive vs. negative	1.75	0.75-4.17	0.201	1.19	0.45-3.13	0.730
Optic nerve involvement						
Positive vs. negative	2.38	1.47-4.00	0.001	1.92	1.11-3.23	0.019

MAGE-A, melanoma antigen-A; RB, retinoblastoma; miR-34a, microRNA-34a; HR, hazard ratio; CI, confidence interval; ICRB, International Classification Of Retinoblastoma.

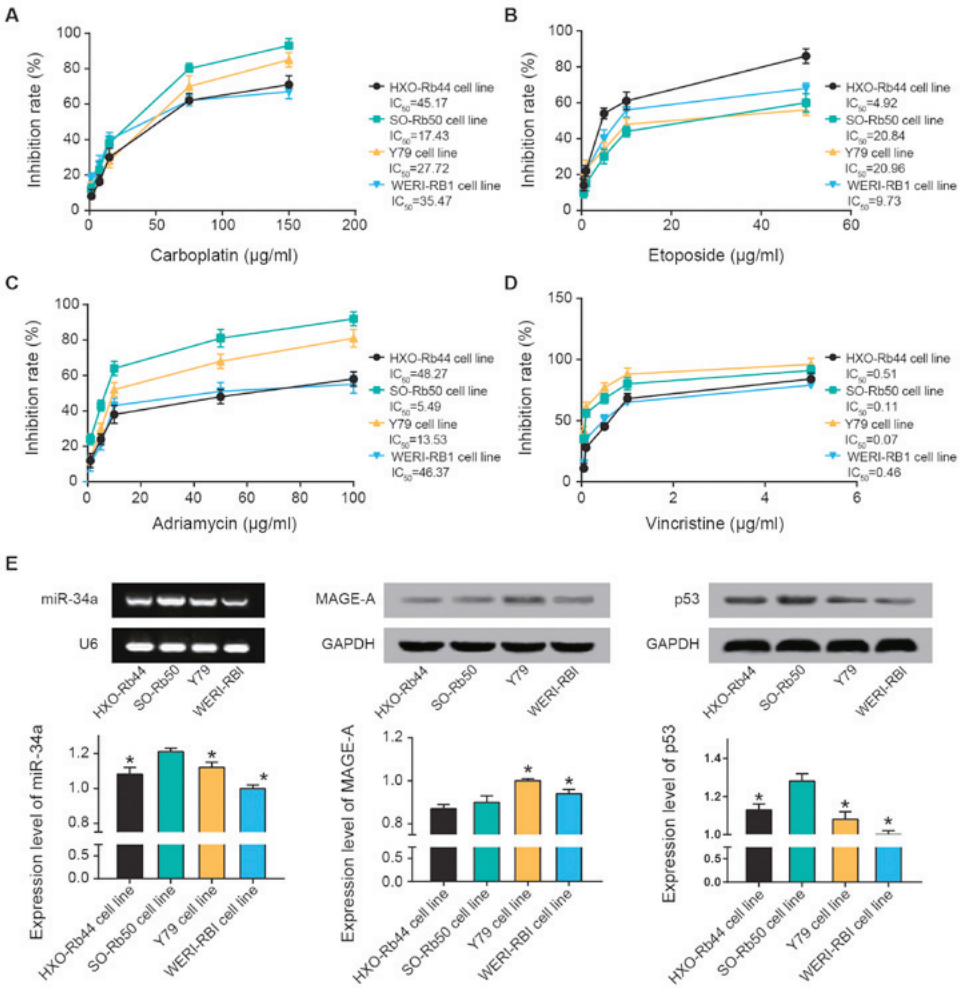

Figure 2. Sensitivities of retinoblastoma cell lines to chemotherapies. Inhibition rates for (A) carboplatin, (B) etoposide, (C) Adriamycin and (D) vincristine were calculated. (E) The expression levels of miR-34a, MAGE-A and p53 were determined in HXO-Rb44, SO-Rb50, Y79 and WERI-RBI cell lines. *P<0.05 compared with the SO-Rb50 cell line. MAGE-A, melanoma antigen-A; miR-34a, microRNA-34a.

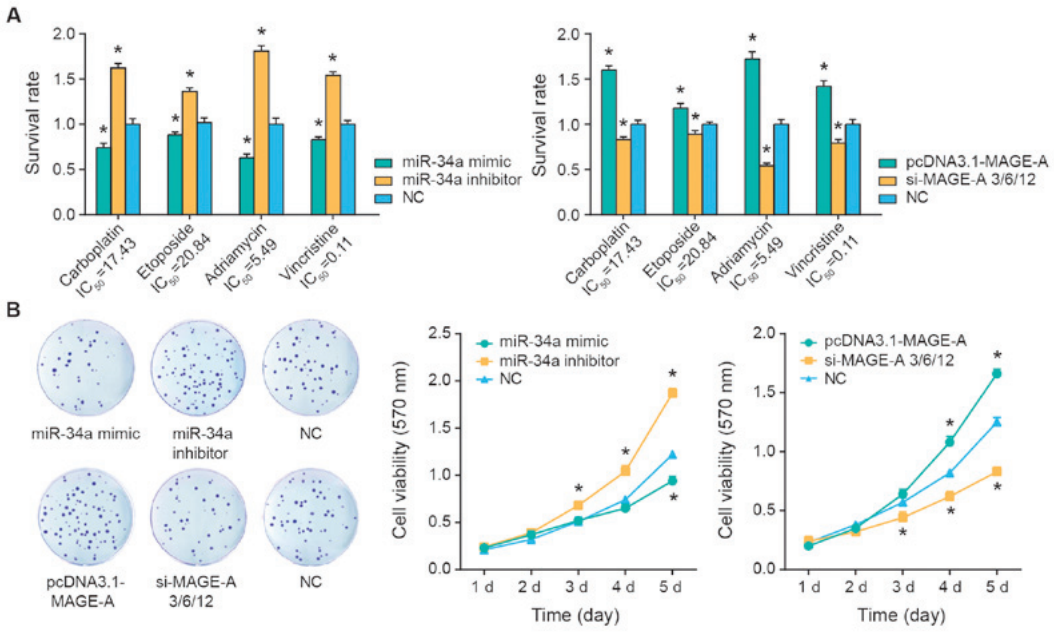

Figure 3. Survival rates and cell viability of retinoblastoma cells. (A) Survival rates of retinoblastoma cells were determined following alterations to miR-34a and MAGE-A expression levels, and treatment with carboplatin, etoposide, Adriamycin and vincristine. (B) The viability rates of retinoblastoma cells following alterations to miR-34a and MAGE-A expression levels were also evaluated. *P<0.05 compared with the NC group. MAGE-A, melanoma antigen-A; miR-34a, microRNA-34a; NC, negative control; si, small interfering RNA.

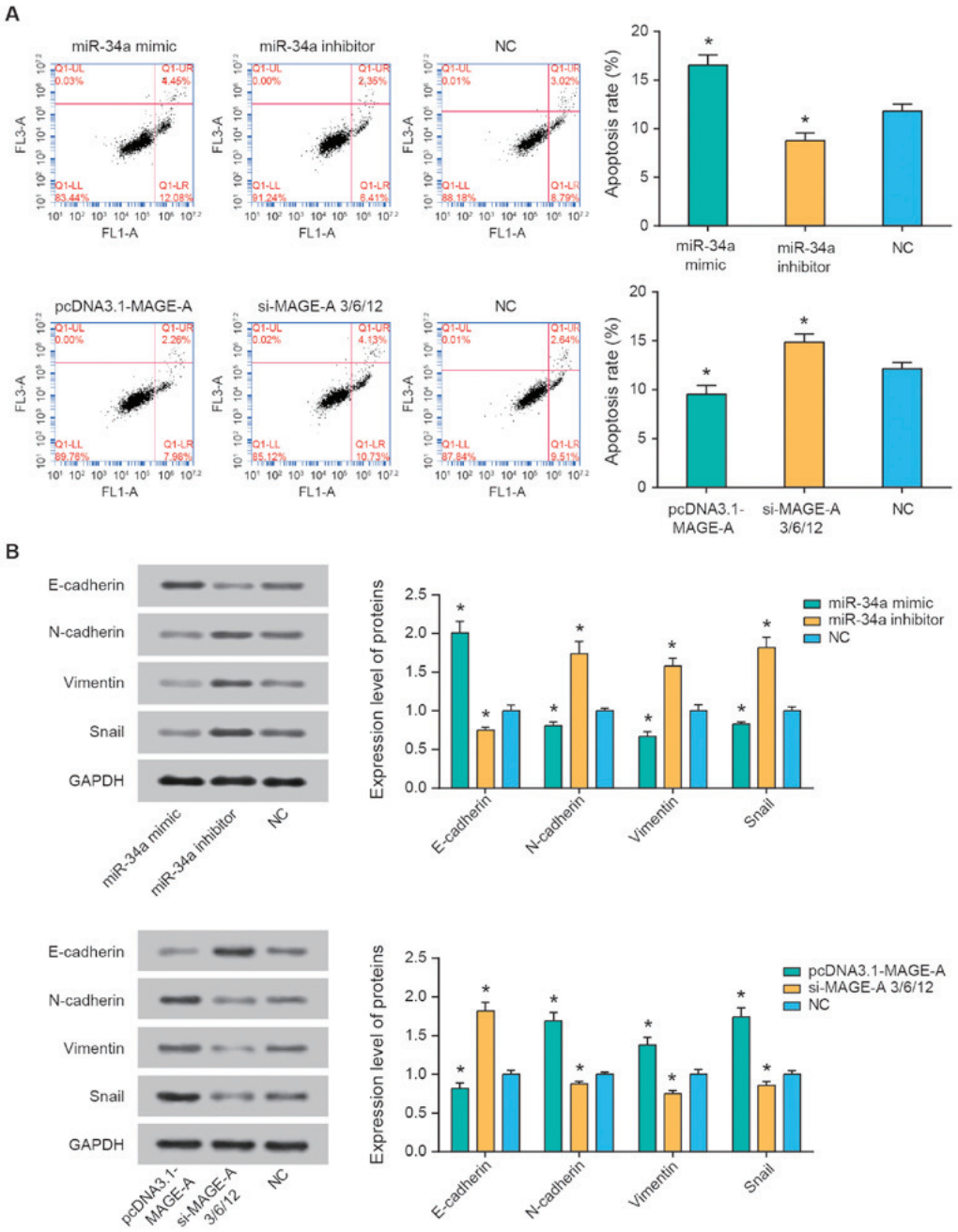

Figure 4. Effects of miR-34a and MAGE-A on apoptosis and EMT. (A) Apoptotic statuses of retinoblastoma cells and (B) the expression of EMT-associated proteins in retinoblastoma cells were assessed following treatments of miR-34a mimic, miR-34a inhibitor, pcDNA3.1-MAGE-A and si-MAGE-A. *P<0.05 compared with the NC group. MAGE-A, melanoma antigen-A; EMT, epithelial-mesenchymal transition; NC, negative control; miR-34a, microRNA-34a; si, small interfering RNA.

Contrary to the results of miR-34a, upregulation of MAGE-A expression was associated with significantly increased survival rates of SO-Rb50 cells in response to carboplatin, etoposide, Adriamycin and vincristine treatment, when compared with the NC group (all P<0.05; Fig. 3A). Concurrently, transfection of si-MAGE-A significantly suppressed the survival rate of SO-Rb50 cells under all four treatment conditions, when compared with the NC group (all P<0.05). In addition, the viability of SO-Rb50 cells was significantly attenuated in the miR-34a mimics and si-MAGE-A groups (P<0.05), while it was significantly improved in the miR-34a inhibitor and pcDNA3-MAGE-A groups compared with the NC group (all P<0.05; Fig. 3B).

miR-34a and MAGE-A regulate epithelial mesenchymal transition (EMT)-specific proteins within RB cells. Flow cytometry was performed to assess the percentage of apoptotic cells and explore the effect of miR-34a and MAGE-A on the apoptotic conditions of SO-Rb50 cells. The results revealed that miR-34a inhibitor and pcDNA3.1-MAGE-A groups significantly reduced the apoptotic rate of SO-Rb50 cells (P<0.05), and the apoptotic rate of miR-34a mimics and si-MAGE-A groups was significantly higher compared with that of the NC group (all P<0.05; Fig. 4A). In addition, as demonstrated in Fig. 4B, miR-34a mimics transfection resulted in increased E-cadherin expression, along with decreased N-cadherin, vimentin and snail expression (all P<0.05),

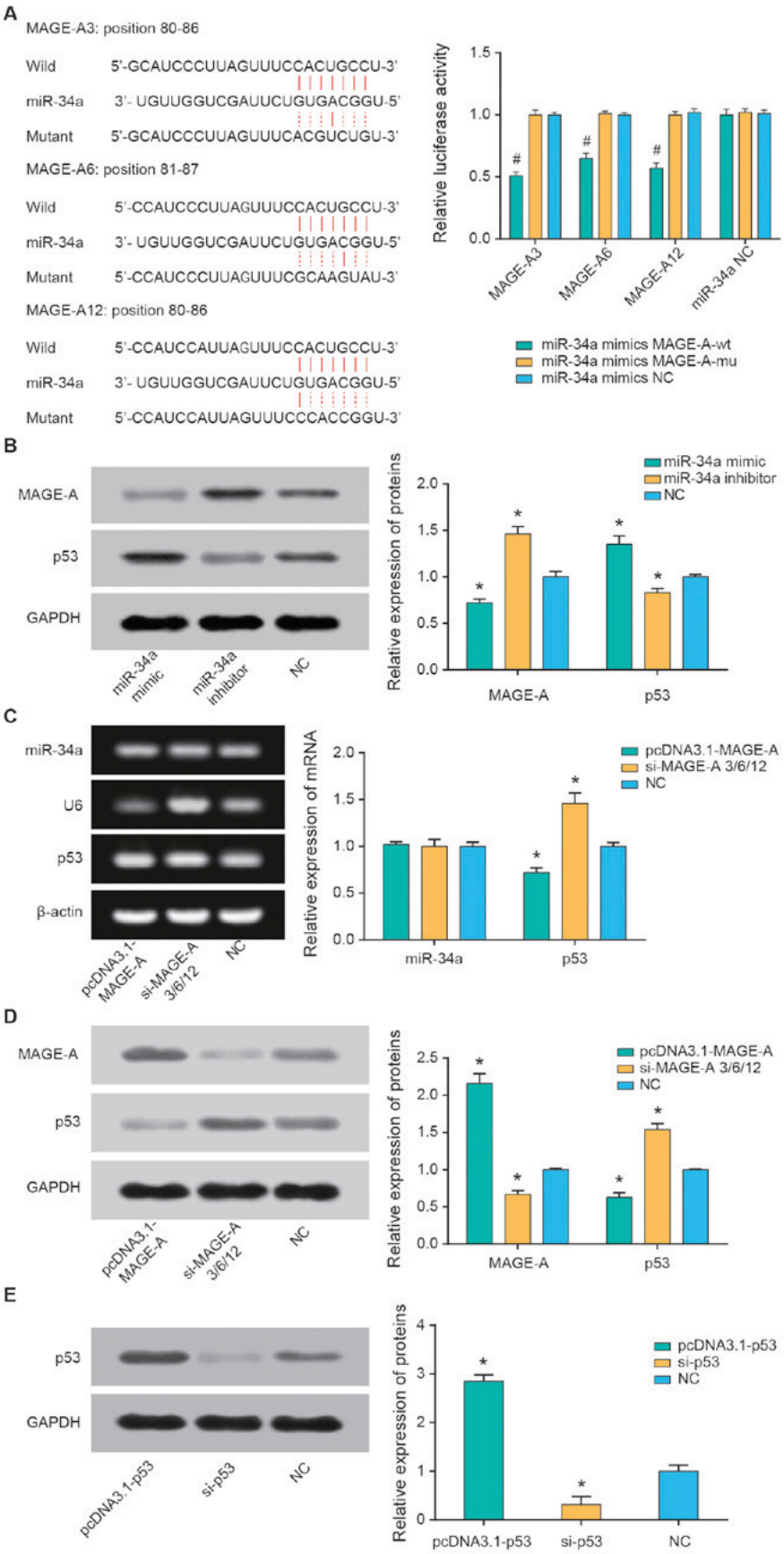

Figure 5. Association among miR-34a, MAGE-A and p53 in retinoblastoma cell lines. (A) The luciferase activities were compared between miR-34a mimics+MAGE-A wt and miR-34a mimics+MAGE-A mut groups. #P<0.05 compared with miR-34a mimics+NC. (B) The effects of miR-34a mimics and miR-34a inhibitor on MAGE-A and p53 expressions were analyzed. (C) The effects of pcDNA3.1-MAGE-A and si-MAGE-A on miR-34a and p53 mRNA expression were compared. (D) The effects of pcDNA3.1-MAGE-A and si-MAGE-A on MAGE-A and p53 protein expression were determined. (E) The effects of pcDNA3.1-p53 and si-p53 on p53 protein expression levels were detected. *P<0.05 compared with the NC group. MAGE-A, melanoma antigen-A; NC, negative control; miR-34a, microRNA-34a; si, small interfering RNA; wt, wild-type; mu, mutant.

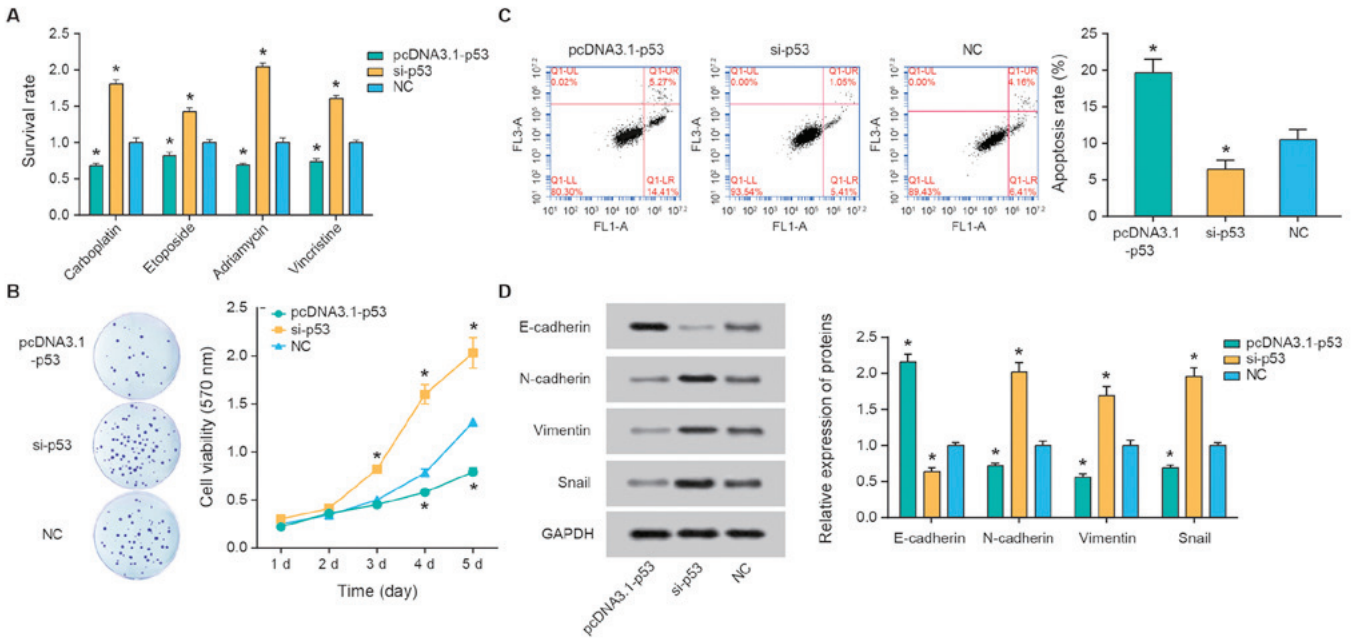

Figure 6. Role of p53 in altering retinoblastoma cell chemosensitivity. (A) The survival rates of retinoblastoma cells were determined following alterations to p53 expression, and treatment with carboplatin, etoposide, Adriamycin and vincristine. (B) The viability and (C) apoptosis statuses of retinoblastoma cells were detected following alteration to p53 expression. (D) The expression of EMT-associated proteins in retinoblastoma cells were evaluated following the upregulation or downregulation of p53 expression. *P<0.05 compared with the NC group. EMT, epithelial-mesenchymal transition; NC, negative control; si, small interfering RNA.

whereas miR-34a inhibitor resulted in the opposite observations (all P<0.05). In addition, treatment with pcDNA3.1-MAGE-A reduced E-cadherin, and increased N-cadherin, vimentin and snail expression levels in SO-Rb50 cells compared with the NC group (all P<0.05). Concurrently, silencing of MAGE-A caused an increase in E-cadherin expression, and a reduction in N-cadherin, vimentin and snail expression levels (all P<0.05).

miR-34a targets MAGE-A to affect the expression of MAGE-A and p53. Based on the TargetScan database, three members of the MAGE-A family (MAGE-A3, MAGE-A6 and MAGE-A12) were identified as the potential targets of miR-34a (Fig. 5A). The double luciferase reporter gene assay was used to further explore whether miR-34a directly binds to the 3'-untranslated region of MAGE-A. miR-34a mimics significantly reduced the luciferase activity in the MAGE-A3, MAGE-A6 and MAGE-A12 groups (all P<0.05), but no significant regulatory effect was observed when MAGE-A3, MAGE-A6 and MAGE-A12 were mutated compared with the NC group (Fig. 5A). Furthermore, transfection with miR-34a mimics significantly decreased MAGE-A and increased p53 expression levels, while miR-34a inhibitor promoted MAGE-A and reduced p53 expression levels (all P<0.05; Fig. 5B). Additionally, overexpression of MAGE-A significantly decreased the mRNA and protein expression of p53 (P<0.05); however, no significant differences were observed regarding the effect of MAGE-A on miR-34a (Fig. 5C and D).

P53 alters RB cell chemosensitivity. p53 expression was significantly upregulated following transfection with pcDNA3.1-p53 and downregulated following si-p53 transfection compared with the NC control (both P<0.05; Fig. 5E). Furthermore, overexpression of p53 was associated with significantly reduced the survival rates of SO-Rb50 cells following treatment with carboplatin, etoposide, Adriamycin and vincristine compared with the NC group (all P<0.05; Fig. 6A). The apoptotic rate of cells in the pcDNA3.1-p53 group was significantly increased compared with the si-p53 group (P<0.05; Fig. 6B), and cell viability in the si-p53 group was increased compared with that in the pcDNA3.1-p53 group (P<0.05; Fig. 6C). Finally, reduced p53 expression resulted in the downregulation of E-cadherin expression, and upregulation of N-cadherin, vimentin and snail expression levels (all P<0.05; Fig. 6D).

Discussion

Accumulating evidence has demonstrated that aberrant expression of miR-34a regulates the progression of various neoplasms (25), including glioma (26), breast cancer (27,28), cervical cancer (29), cholangiocarcinoma (30) and multiple myeloma (31). The results of the present study demonstrated that the expression level of miR-34a was reduced in RB tissues compared with that in paracarcinoma tissues (P<0.05). Generally, miRNAs modulate diverse biological processes by targeting downstream mRNA (32-34). For instance, miR-34a has been reported to regulate carcinogenesis by targeting several mRNAs, including MAGE-A in medulloblastoma (22), programmed cell death 1 ligand 1 or lactate dehydrogenase A in breast cancer (28), and B cell lymphoma-2 in cervical cancer (29). The expression of MAGE-A has been documented to be upregulated in gastric cancer (35), epithelial ovarian cancer (36), and lung adenocarcinoma tissues and cells (37). In agreement with the aforementioned studies, the results of the RT-qPCR analysis in the present study revealed that the mRNA level of MAGE-A was significantly upregulated in RB tissues compared with paracarcinoma tissues (P<0.05). The clinical studies also indicated that high MAGE-A expression and low miR-34a expression were significantly associated with poor

prognosis of patients with RB (P<0.05). Furthermore, in order to investigate the role of miR-34a and MAGE-A underlying RB etiology, their binding sites were predicted using the Targetscan database, and validated their targeted association by performing a dual luciferase reporter gene assay. The results of the current study also suggested that MAGE-A expression in SO-Rb50 cells was significantly reduced following transfection with miR-34a mimics and increased following miR-34a inhibitor transfection. Collectively, these results suggested that the downregulation of MAGE-A by miR-34a partially mediated the pathogenesis of RB.

Furthermore, the aforementioned carcinogenic mechanism of miR-34a and MAGE-A in RB was hypothesized to be the result of their contribution to enhancing cell viability and modulating cell apoptosis (38-41). In the present study, miR-34a mimics, miR-34a inhibitor or pCDNA3-MAGE-A were transfected into SO-Rb50 cells, and their effects on viability, survival rate and apoptosis of SO-Rb50 were analyzed. The results revealed that the addition of miR-34a mimics and silencing of MAGE-A significantly suppressed cell viability and cell survival, and induced apoptosis. Furthermore, significantly increased E-cadherin expression, as well as decreased N-cadherin, vimentin and snail expression levels were observed in SO-Rb50 cells. Additionally, the transfection of miR-34a inhibitor and pcDNA3.1-MAGE-A were able to impede the apoptosis of SO-Rb50 cells, and encourage its viability and survival. It may be concluded that miR-34a, through targeting MAGE-A, is involved in RB pathogenesis by altering cell survival, cell viability, cell apoptosis and expression levels of EMT-associated proteins.

Furthermore, miR-34a and MAGE-A were demonstrated to regulate p53 expression, SO-Rb50 cell viability, survival and apoptotic rates, as well as E-cadherin, N-cadherin, vimentin and snail expression levels. p53 serves as a transcription factor that is largely involved in cell growth, cell differentiation, cell senescence and cell apoptosis (38,42-44). In addition, it has been previously suggested that the inhibitory effects of MAGE-A on p53 transactivation may lead to tumor cell resistance to chemotherapeutic drugs (etoposide) (45). miR-34a confers chemosensitivity of medulloblastoma cells through modulation of MAGE-A and p53 expression levels (22). Similar to the aforementioned publications, the present study demonstrated that miR-34a, MAGE-A and p53 were able to significantly alter the resistance of SO-Rb50 cells to vincristine, etoposide, carboplatin and Adriamycin. Taken together, the results suggest that miR-34a targeted MAGE-A and thereby regulated MAGE-A to alter the chemosensitivity of RB cells, and this phenomenon was achieved possibly through alterations to the viability, survival, apoptosis and EMT of RB cells.

In conclusion, miR-34a may function as a tumor suppressor for RB by targeting MAGE-A and altering p53 expression, indicating that the miR-34a/MAGE-A/p53 axis may serve as a therapeutic target or diagnostic biomarker for RB. However, a number of limitations must be addressed. Firstly, the results may not well be generalized to other ethnicities or a larger population, due to the limited sample size incorporated in the present study. Secondly, only the SO-Rb50 cell line was examined, and more cell lines should be focused on to verify the mechanisms. Thirdly, no animal models were established, which may provide a direct understanding regarding the influence of the miR-34a/MAGE-A/p53 axis on RB development. Lastly, long non-coding RNAs and circular RNAs are situated upstream of miRNAs, and may also participate in the mechanism underlying RB carcinogenesis. As a result, further studies are required to explore the molecular mechanism of the miR-34a/MAGE-A/p53 axis on RB progression.

Acknowledgements

Not applicable.

Funding

The present study was supported by Chinese National Natural Science Foundation of Youth Fund (grant no. 81602154), the Technology Research Projects of Henan Science and Technology Department (grant nos. 162102410060 and 182107000054), Outstanding Young Talent Research Fund of Zhengzhou University (grant no. 1621328002) and the Special Funding for Doctoral Team of the First Affiliated Hospital of Zhengzhou University (grant no. 2016-BSTDJJ-11).

Availability of data and materials

All data generated or analyzed during this study are included in this article.

Authors' contributions

GY, YF, XL, MW, HD and QL conceived and designed the experiments, performed the experiments. GY, YF, XL and MW analyzed the data. HD and QL drafted the manuscript. All authors read and approved the final manuscript.

Ethics approval and consent to participate

The immediate relatives of all patients with RB provided written informed consent, and the present study was approved by the Ethics Committee of The First Affiliated Hospital of Zhengzhou University.

Patient consent for publication

The immediate relatives of all patients with RB provided written informed consent.

Competing interests

The authors declare that they have no competing interests.

References

1. Aerts I, Lumbroso-Le Rouic L, Gauthier-Villars M, Brisse H, Doz F and Desjardins L: Retinoblastoma. Orphanet J Rare Dis 1: 31, 2006.
2. Kivelä T: The epidemiological challenge of the most frequent eye cancer: Retinoblastoma, an issue of birth and death. Br J Ophthalmol 93: 1129-1131, 2009.
3. Shields CL, Fulco EM, Arias JD, Alarcon C, Pellegrini M, Rishi P, Kaliki S, Bianciotto CG and Shields JA: Retinoblastoma frontiers with intravenous, intra-arterial, periocular, and intravitreal chemotherapy. Eye (Lond) 27: 253-264, 2013.

4. Abramson DH, Gerardi CM, Ellsworth RM, McCormick B, Sussman D and Turner L: Radiation regression patterns in treated retinoblastoma: 7 to 21 years later. J Pediatr Ophthalmol Strabismus 28: 108-112, 1991.
5. Fontanesi J, Pratt CB, Hustu HO, Coffey D, Kun LE and Meyer D; Jude Children's Research Hospital Experience and Review of Literature: Use of irradiation for therapy of retinoblastoma in children more than 1 year old: The St. Jude Children's Research Hospital experience and review of literature. Med Pediatr Oncol 24: 321-326, 1995.
6. Shields CL, Say EA, Pointdujour-Lim R, Cao C, Jabbour PM and Shields JA: Rescue intra-arterial chemotherapy following retinoblastoma recurrence after initial intra-arterial chemotherapy. J Fr Ophtalmol 38: 542-549, 2015.
7. Ruiz del Río N, Abelairas Gómez JM, Alonso García de la Rosa FJ, Peralta Calvo JM and de las Heras Martín A: Genetic analysis results of patients with a retinoblastoma refractory to systemic chemotherapy. Arch Soc Esp Oftalmol 90: 414-420, 2015 (In Spanish).
8. Nalini V, Segu R, Deepa PR, Khetan V, Vasudevan M and Krishnakumar S: Molecular insights on post-chemotherapy retinoblastoma by microarray gene expression analysis. Bioinform Biol Insights 7: 289-306, 2013.
9. Frankel LB and Lund AH: MicroRNA regulation of autophagy. Carcinogenesis 33: 2018-2025, 2012.
10. Tazawa H, Tsuchiya N, Izumiya M and Nakagama H: Tumor-suppressive miR-34a induces senescence-like growth arrest through modulation of the E2F pathway in human colon cancer cells. Proc Natl Acad Sci USA 104: 15472-15477, 2007.
11. Tarasov V, Jung P, Verdoodt B, Lodygin D, Epanchintsev A, Menssen A, Meister G and Hermeking H: Differential regulation of microRNAs by p53 revealed by massively parallel sequencing: miR-34a is a p53 target that induces apoptosis and G1-arrest. Cell Cycle 6: 1586-1593, 2007.
12. Sun F, Fu H, Liu Q, Tie Y, Zhu J, Xing R, Sun Z and Zheng X: Downregulation of CCND1 and CDK6 by miR-34a induces cell cycle arrest. FEBS Lett 582: 1564-1568, 2008.
13. Yamakuchi M, Ferlito M and Lowenstein CJ: miR-34a repression of SIRT1 regulates apoptosis. Proc Natl Acad Sci USA 105: 13421-13426, 2008.
14. Ma ZB, Kong XL, Cui G, Ren CC, Zhang YJ, Fan SJ and Li YH: Expression and clinical significance of miRNA-34a in colorectal cancer. Asian Pac J Cancer Prev 15: 9265-9270, 2014.
15. Liu G, Jiang C, Li D, Wang R and Wang W: miRNA-34a inhibits EGFR-signaling-dependent MMP7 activation in gastric cancer. Tumour Biol 35: 9801-9806, 2014.
16. Dalgard CL, Gonzalez M, deNiro JE and O'Brien JM: Differential microRNA-34a expression and tumor suppressor function in retinoblastoma cells. Invest Ophthalmol Vis Sci 50: 4542-4551, 2009.
17. Gao H, Zhao H and Xiang W: Expression level of human miR-34a correlates with glioma grade and prognosis. J Neurooncol 113: 221-228, 2013.
18. Li L, Yuan L, Luo J, Gao J, Guo J and Xie X: miR-34a inhibits proliferation and migration of breast cancer through down-regulation of Bcl-2 and SIRT1. Clin Exp Med 13: 109-117, 2013.
19. Tang Y, Tang Y and Cheng YS: miR-34a inhibits pancreatic cancer progression through Snail1-mediated epithelial-mesenchymal transition and the Notch signaling pathway. Sci Rep 7: 38232, 2017.
20. Vinall RL, Ripoll AZ, Wang S, Pan CX and deVere White RW: miR-34a chemosensitizes bladder cancer cells to cisplatin treatment regardless of p53-Rb pathway status. Int J Cancer 130: 2526-2538, 2012.
21. Kang L, Mao J, Tao Y, Song B, Ma W, Lu Y, Zhao L, Li J, Yang B and Li L: MicroRNA-34a suppresses the breast cancer stem cell-like characteristics by downregulating Notch1 pathway. Cancer Sci 106: 700-708, 2015.
22. Weeraratne SD, Amani V, Neiss A, Teider N, Scott DK, Pomeroy SL and Cho YJ: miR-34a confers chemosensitivity through modulation of MAGE-A and p53 in medulloblastoma. Neuro-oncol 13: 165-175, 2011.
23. Peche LY, Scolz M, Ladelfa MF, Monte M and Schneider C: MageA2 restrains cellular senescence by targeting the function of PMLIV/p53 axis at the PML-NBs. Cell Death Differ 19: 926-936, 2012.
24. Nardiello T, Jungbluth AA, Mei A, , Diliberto M, Huang X, Dabrowski A, Andrade VC, Wasserstrum R, Ely S, Niesvizky R, *et al*: MAGE-A inhibits apoptosis in proliferating myeloma cells through repression of Bax and maintenance of survivin. Clin Cancer Res 17: 4309-4319, 2011.
25. Krauskopf J, de Kok TM, Hebels DG, Bergdahl IA, Johansson A, Spaeth F, Kiviranta H, Rantakokko P, Kyrtopoulos SA and Kleinjans JC: MicroRNA profile for health risk assessment: Environmental exposure to persistent organic pollutants strongly affects the human blood microRNA machinery. Sci Rep 7: 9262, 2017.
26. Jin Z, Zhan T, Tao J, Xu B, Zheng H, Cheng Y, Yan B, Wang H, Lu G, Lin Y, *et al*: MicroRNA-34a induces transdifferentiation of glioma stem cells into vascular endothelial cells by targeting Notch pathway. Biosci Biotechnol Biochem 81: 1899-1907, 2017.
27. Engkvist ME, Stratford EW, Lorenz S, Meza-Zepeda LA, Myklebost O and Munthe E: Analysis of the miR-34 family functions in breast cancer reveals annotation error of miR-34b. Sci Rep 7: 9655, 2017.
28. Huang X, Xie X, Wang H,, Xiao X, Yang L, Tian Z, Guo X, Zhang L, Tang H and Xie X: PDL1 And LDHA act as ceRNAs in triple negative breast cancer by regulating miR-34a. J Exp Clin Cancer Res 36: 129, 2017.
29. Wang X, Xie Y and Wang J: Overexpression of microRNA-34a-5p inhibits proliferation and promotes apoptosis of human cervical cancer cells by downregulation of Bcl-2. Oncol Res: Aug 30, 2017 (Epub ahead of print). doi: 10.3727/096504017X15037506066252.
30. Kwon H, Song K, Han C, Zhang J, Lu L, Chen W and Wu T: Epigenetic silencing of miRNA-34a in human cholangiocarcinoma via EZH2 and DNA methylation: Impact on regulation of notch pathway. Am J Pathol 187: 2288-2299, 2017.
31. Dai X, Li M and Geng F: Omega-3 polyunsaturated fatty acids eicosapentaenoic acid and docosahexaenoic acid enhance dexamethasone sensitivity in multiple myeloma cells by the p53/miR-34a/Bcl-2 axis. Biochemistry (Mosc) 82: 826-833, 2017.
32. Ritchie W, Rasko JE and Flamant S: MicroRNA target prediction and validation. Adv Exp Med Biol 774: 39-53, 2013.
33. Witkos TM, Koscianska E and Krzyzosiak WJ: Practical aspects of microRNA target prediction. Curr Mol Med 11: 93-109, 2011.
34. Zheng L, Zhang Y, Liu Y, Zhou M, Lu Y, Yuan L, Zhang C, Hong M, Wang S and Li X: miR-106b induces cell radioresistance via the PTEN/PI3K/AKT pathways and p21 in colorectal cancer. J Transl Med 13: 252, 2015.
35. Lian Y, Sang M, Gu L, Liu F, Yin D, Liu S, Huang W, Wu Y and Shan B: MAGE-A family is involved in gastric cancer progression and indicates poor prognosis of gastric cancer patients. Pathol Res Pract 213: 943-948, 2017.
36. Sang M, Wu X, Fan X, Lian Y and Sang M: MAGE-A family serves as poor prognostic markers and potential therapeutic targets for epithelial ovarian cancer patients: A retrospective clinical study. Gynecol Endocrinol 33: 480-484, 2017.
37. Sang M, Gu L, Yin D, Liu F, Lian Y, Zhang X, Liu S, Huang W, Wu Y and Shan B: MAGE-A family expression is correlated with poor survival of patients with lung adenocarcinoma: A retrospective clinical study based on tissue microarray. J Clin Pathol 70: 533-540, 2017.
38. Marcar L, Maclaine NJ, Hupp TR and Meek DW: Mage-A cancer/testis antigens inhibit p53 function by blocking its interaction with chromatin. Cancer Res 70: 10362-10370, 2010.
39. Zajac P, Schultz-Thater E, Tornillo L, Sadowski C, Trella E, Mengus C, Iezzi G and Spagnoli GC: MAGE-A antigens and cancer immunotherapy. Front Med (Lausanne) 4: 18, 2017.
40. Sato F, Tsuchiya S, Meltzer SJ and Shimizu K: MicroRNAs and epigenetics. FEBS J 278: 1598-1609, 2011.
41. Huang Y, Shen XJ, Zou Q, Wang SP, Tang SM and Zhang GZ: Biological functions of microRNAs: A review. J Physiol Biochem 67: 129-139, 2011.
42. Kircelli F, Akay C and Gazitt Y: Arsenic trioxide induces p53-dependent apoptotic signals in myeloma cells with SiRNA-silenced p53: MAP kinase pathway is preferentially activated in cells expressing inactivated p53. Int J Oncol 30: 993-1001, 2007.
43. Riley T, Sontag E, Chen P and Levine A: Transcriptional control of human p53-regulated genes. Nat Rev Mol Cell Biol 9: 402-412, 2008.
44. Vousden KH and Prives C: Blinded by the light: The growing complexity of p53. Cell 137: 413-431, 2009.
45. Monte M, Simonatto M, Peche LY, Bublik DR, Gobessi S, Pierotti MA, Rodolfo M and Schneider C: MAGE-A tumor antigens target p53 transactivation function through histone deacetylase recruitment and confer resistance to chemotherapeutic agents. Proc Natl Acad Sci USA 103: 11160-11165, 2006.